PHYSICAL REVIEW B **92**, 161301(R) (2015)

# Electron $g$-factor anisotropy in an AlAs quantum well probed by ESR

A. V. Shchepetilnikov,[1,2,*] Yu. A. Nefyodov,[1] I. V. Kukushkin,[1] L. Tiemann,[3] C. Reichl,[3] W. Dietsche,[3] and W. Wegscheider[3]

[1]*Institute of Solid State Physics RAS, 142432 Chernogolovka, Moscow District, Russia*

[2]*Moscow Institute of Physics and Technology, 141700 Dolgoprudny, Russia*

[3]*Solid State Physics Laboratory, ETH Zurich, Schafmattstrasse 16, 8093 Zurich, Switzerland*

(Received 4 August 2015; published 8 October 2015)

Electron spin resonance (ESR) was studied in an asymmetrically doped 16-nm AlAs quantum well grown in the [001] direction. Surprisingly the ESR was detectable even if the magnetic field was parallel to the surface of the two-dimensional system. This allowed us to investigate precisely the in-plane anisotropy of the electron $g$ factor. In the case of the magnetic field aligned along the [110] or [1$\bar{1}$0] crystallographic axes only one ESR peak was observed, whereas it tended to split into two well-separated peaks when the in-plane component of the magnetic field was between these directions. This fact clearly indicates that two in-plane valleys at $X$ points of the Brillouin zone were occupied with electrons and each valley was characterized by the anisotropic $g$ factor with the [100], [010], and [001] principal axes. The principal $g$-factor values were extracted.

DOI: 10.1103/PhysRevB.92.161301 PACS number(s): 73.43.Lp, 73.43.Qt

Electron-electron interactions are responsible for a vast amount of beautiful physical phenomena in two-dimensional (2D) electron systems. Fractional quantum Hall effect [1], Wigner crystallization [2], and Stoner instability [3] are among the most prominent and well-known many-particle effects. The key parameter that describes the strength of the electron-electron correlations is $r_s$—the ratio of characteristic Coulomb energy to the Fermi energy. Numerically $r_s$ can be expressed as $\frac{1}{\sqrt{\pi n_s}}\frac{m^* e^2}{\epsilon \hbar^2}$, where $n_s$ is the sheet electron density, $m^*$ is the effective electron mass, and $\epsilon$ is the dielectric constant. In typical AlAs quantum wells the effective mass of the electrons [4] is heavier by an order of magnitude, and thus the $r_s$ parameter is higher than in GaAs heterostructures. This implies that many-particle effects are significantly more pronounced in AlAs-based heterostructures so that, e.g., fractional Hall effect can be observed [5]. In particular spin properties are susceptible to this interaction when it surmounts the spin splitting, i.e., an energy that depends on the $g$ factor of the material. This evokes great fundamental interest in systems with strong many-particle effects. The present paper is aiming to study the significant electron $g$-factor anisotropy in the asymmetrical AlAs quantum well grown in the [001] direction with the aid of the electron spin resonance (ESR) technique.

In the bulk AlAs semiconductor the minima of the conduction band lay at the $X$ points, i.e., the points at the edge of the Brillouin zone along the [100], [010], and [001] crystallographic axes. These valleys are commonly referred to as the $X$ valley for the [100] direction, the $Y$ valley for the [010], and the $Z$ valley for the [001] directions. The schematic of the electron valley positions with respect to the in-plane crystallographic axes is shown in the inset to Fig. 1. In relatively narrow AlAs quantum wells grown in the [001] direction only the $Z$ valley is occupied, whereas in wells wider than 5 nm electrons tend to populate in-plane valleys instead. The electron population of the $X$ and $Y$ valleys can be unequal and depends on the sample structure and applied strain [4]. The width of the quantum well under study is 16 nm and, thus, we will focus on the case when the in-plane valleys are occupied. Although in bulk AlAs all three electron valleys are characterized by a highly anisotropic mass with the ratio of longitudinal to transverse effective masses larger than 5, the effective $g^*$ factor is close to the free electron value $g^* \approx 1.98$ [6] and is isotropic [7]. Thus the electron $g$-factor tensor is simply a scalar. Spatial confinement in the [001] direction reduces the symmetry of the system, and in the case of the asymmetric confining potential one can expect the $g$-factor tensor in the $X$ and $Y$ valleys to be characterized by three independent components. If for a certain orientation of the magnetic field the effective $g$ factors of the $X$ and $Y$ valleys do not coincide, two separate spin resonances can be observed.

The situation described above is quite similar to the $g$-factor behavior in GaAs-based heterostructures, namely, the electron $g$ factor is isotropic in bulk GaAs but becomes strongly anisotropic in GaAs quantum wells [8–11]. One might even expect the same mechanisms of the $g$-factor anisotropy discovered for GaAs quantum wells [12–14] to hold true for the case of AlAs heterostructures.

The aim of the present Rapid Communication is to investigate thoroughly the in-plane and out-of-plane anisotropies of the $g$ factor in an asymmetrically doped 16-nm AlAs/AlGaAs quantum well grown in the [001] direction to determine experimentally the principal axes and carefully measure all three components of the electron $g$-factor tensor. The experimental approach based on the electrically detected ESR appears to be the most suitable for this task. This technique is based on the strong sensitivity of the longitudinal magnetoresistance $\rho_{xx}(B)$ of the two-dimensional electron gas (2DEG) to the spin resonance in the quantum Hall regime. The ESR can be detected as a sharp peak in $\rho_{xx}(B)$ magnetic-field dependence at a fixed rf frequency. This experimental technique was first proposed in 1983 [15] and since then has been successfully utilized to study the spin properties of many 2DEG systems. In our previous works [10,11,14] we applied this approach to carefully investigate the $g$-factor anisotropy in GaAs-based heterostructures.

Surprisingly, the conventional resonator technique of ESR detection turned out to be applicable to AlAs-based heterostructures [6]. With the aid of this technique spin resonance was shown to originate not from the microwave magnetic field, but from the effective magnetic field due to spin-orbit

*shchepetilnikov@issp.ac.ru

 

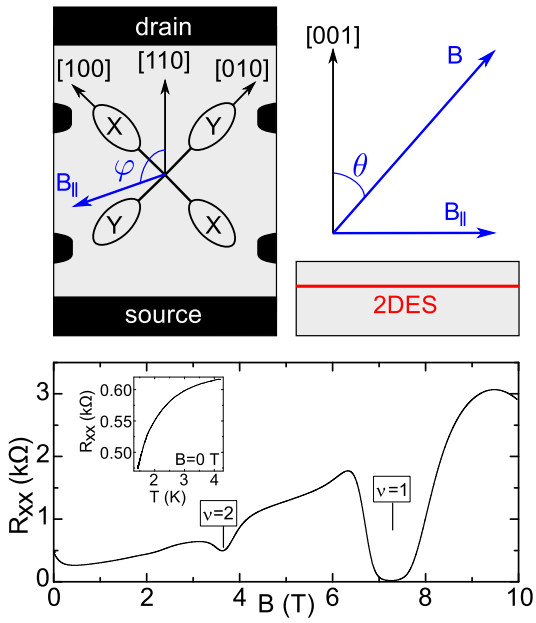


FIG. 1. (Color online) The schematic of the electron valley's position with respect to the in-plane crystallographic axes in the AlAs quantum well is presented in the upper panel. The lower panel shows the longitudinal resistance of the sample measured in the perpendicular magnetic field at the temperature of 1.4 K. Inset to the lower panel: temperature dependence of the sample longitudinal resistance at zero magnetic field.

interaction and modulation of the electron wave vector by the microwave electric field. However, no thorough studies of the electron $g$ factor were performed in that paper, so the present Rapid Communication measures the electron $g$-factor anisotropy in AlAs-based heterostructures. Let us note that detection of the spin resonance as a resistance peak is much more convenient for the experiments in a wide range of rf frequencies at low temperatures than the conventional resonator-based technique.

The electron $g$ factor acquired with the aid of the ESR technique is substantially single particle since the Larmour theorem prohibits any contribution from the electron-electron interactions to the value of the measured spin splitting and, thus, the $g$ factor. This fact was also confirmed by theoretical calculations [16].

We have studied a 16-nm AlAs quantum well which was epitaxially grown along the [001] direction. The Al concentration in the $Al_xGa_{1-x}As$ barrier layers was equal to 46%. The structure was asymmetrically $\delta$ doped with Si to result in a low-temperature sheet density of $n \approx 1.8 \times 10^{11}$ cm$^{-2}$. The spacer layer between the quantum well and the doping layer was 35-nm thick. The electron mobility was equal to $2 \times 10^5$ cm$^2$ V$^{-1}$ s$^{-1}$ at a temperature of 1.4 K. Standard indium contacts to the 2D electron system were formed in the common Hall bar geometry.

An ac probe current of 1 $\mu$A at a frequency of $\sim$1 kHz was applied from source to drain. A lock-in amplifier monitored the channel resistance $R_{xx}$ through two sense contacts along the channel. The sample was irradiated by 100% amplitude modulated radiation at a frequency of $f_{mod}\sim$30 Hz; rf power was delivered through a rectangular oversized waveguide. A second lock-in amplifier, synchronized at $f_{\rm mod}$ frequency, was connected to the output of the first one and, thus, measured the variation $\delta R_{xx}$ in the magnetoresistance, caused by microwave irradiation. The sample was mounted on the rotation stage so that we were able to change the orientation of the magnetic field with respect to the sample crystallographic axes. The angle between the in-plane component of the magnetic field and the [110] direction is referred to as $\varphi$. The angle between the normal to the 2DEG plane and the magnetic field is denoted as $\theta$. Both angles $\theta$ and $\varphi$ could be changed and monitored with the aid of the three-dimensional magnetic field sensor rigidly attached to the sample.

The hyperfine interaction of electron and nuclear spins commonly causes dynamic polarization of nuclear spins in GaAs-based heterostructures and complicates the precise measurements of the electron $g$ factor by shifting the position and changing the shape of the ESR line [17,18]. Rather slight dynamic polarization of nuclear spins was observed under certain conditions, which will be discussed in more detail in a separate publication. The data obtained in this Rapid Communication showed no sign of nuclear polarization.

The longitudinal resistance of the sample measured in the perpendicular magnetic field ($\theta = 0$) at the temperature of 1.4 K is shown in the lower panel of Fig. 1. The upper panel shows schematically the electron valley's position with respect to the in-plane crystallographic axes.

Surprisingly, the ESR did not vanish in the case of $\theta = 90^\circ$. This may be ascribed to the fact that even at zero out-of-plane magnetic field where no Landau quantization takes place, the longitudinal resistance of the sample demonstrated temperature dependence strong enough to allow for the detection of even subtle heating of the electron system caused by the resonant microwave absorption. Temperature dependence of the resistance at zero magnetic field is presented in the inset to the lower panel of Fig. 1. The value of the electron $g$ factor was so large that the rf frequency at which ESR occurred (in the magnetic-field range of 2–6 T) was well above the temperature at which the experiment was conducted so that the electron system would be spin polarized to a rather high degree.

The typical ESR peaks in $\delta R_{xx}$ measured for a fixed frequency of $f = 120$ GHz of microwave radiation and different angles $\varphi$ are presented in Fig. 2. The angle $\theta$ was equal to 90°, i.e., the magnetic field $B$ was parallel to the plane of the 2DEG. All peaks are of the Lorentzian line shape. The single ESR peak was observed for the case of $\varphi = 0^\circ$ or 90° (magnetic field oriented along the [110] or $1\bar{1}0$ axes), however it splits into two well-separated resonance lines for other $\varphi$ angles. The maximal separation between the two peaks is achieved when angle $\varphi = 45^\circ, 135^\circ, \ldots$, i.e., the magnetic field is directed along the [100] or [010] axes. We believe these two spin resonances to originate from the $X$ and $Y$ valleys populated with electrons. Apparently, the $Z$ valley was empty of the electrons in our sample as the position of the correspondent resonance line should have been independent of angle $\varphi$. Moreover, only one resonance was detected in the case of $\theta = 0^\circ$. From the inset to Fig. 1 it can be clearly seen that the system symmetry dictates that the electron $g$ factors of the populated valleys should be equal for the [110] or [$1\bar{1}0$] directions, and thus, spin resonances originating

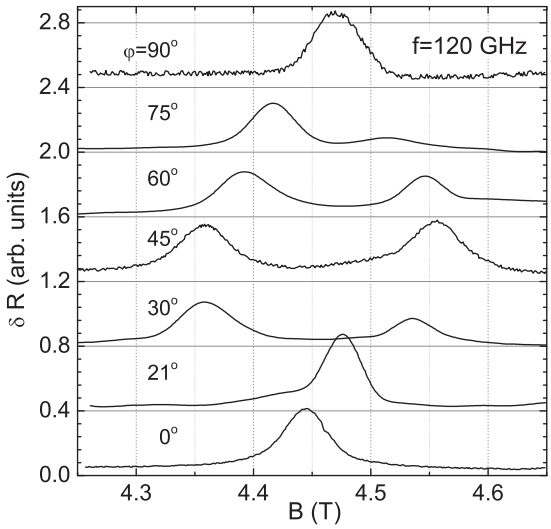


FIG. 2. Typical ESR peaks measured at different orientations of the in-plane magnetic field (data shifted for clarity). Angle $\theta$ was fixed at 90°, temperature was 1.4 K, and microwave radiation frequency was equal to 120 GHz.

from these valleys should overlap into a single peak. For the same symmetrical reasons the maximal difference between the electron $g$ factors of the $X$ and $Y$ valleys (and, as a result, the maximal separation between ESR peaks) is to be observed in the case of $B$ directed along [100] or [010].

To study the electron $g$ factor more precisely we measured the ESR for a vast set of experimentally accessible microwave frequencies $f$ with angles $\theta$ and $\varphi$ fixed. In the case of $\varphi \neq 0°,90°$ and $\theta \neq 0°$ two distinct ESR peaks were observed for all the frequencies, and thus two magnetic fields $B_1$ and $B_2$ were obtained for a single $f$ yielding two separate dependences $f(B_1)$ and $f(B_2)$. All of the thus acquired dependences $f(B_1)$ and $f(B_2)$ could be ideally fitted with a linear expression $f = f_0 + \alpha B$ with negligibly small $f_0$. This is illustrated by Fig. 3 where $f(B)$ dependences of the lower and upper

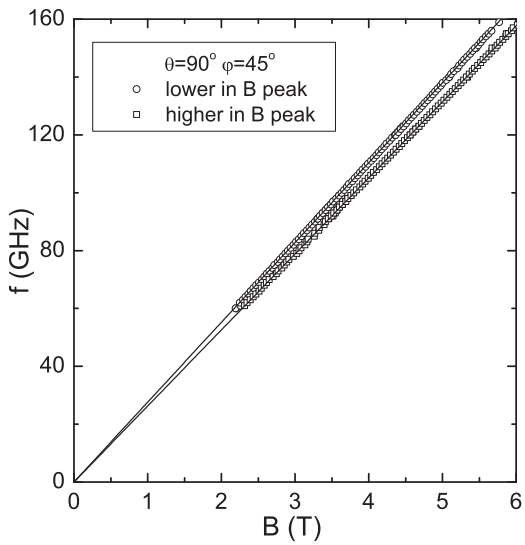


FIG. 3. $f(B)$ dependences of the lower and upper in the magnetic-field peaks for the cases of $\theta = 90°$, $\varphi = 45°$.

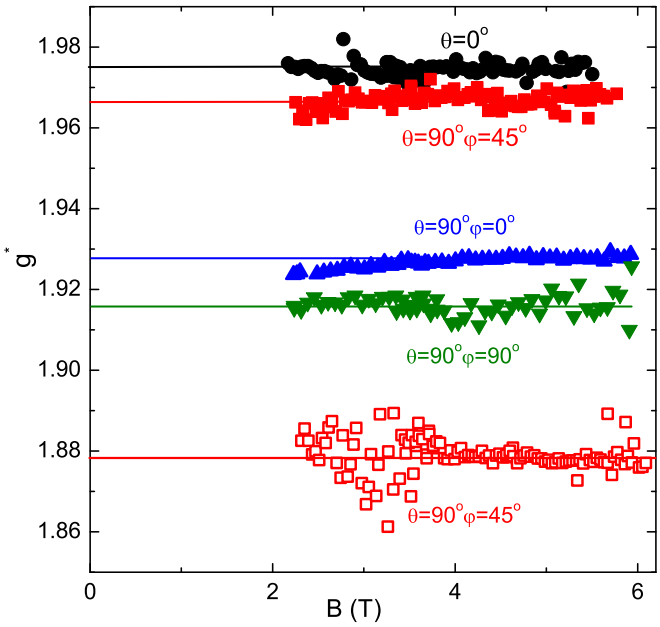


FIG. 4. (Color online) The dependences of the effective $g$ factor on the magnetic field for several most important magnetic-field orientations with respect to the crystallographic axes of the sample. Solid lines represent linear extrapolations to zero magnetic field.

peaks are shown for the cases of $\theta = 0°$, $\varphi = 45°$. These dependences are close to each other, however the difference between them is much higher than the experimental error. This fact together with the smallness of $f_0$ for all the fits allow us to extract two separate electron $g$-factor dependences $g_1(B_1) = \frac{f(B_1)}{\mu_B B_1}$ and $g_2(B_2) = \frac{f(B_2)}{\mu_B B_2}$, where $\mu_B$ is the Bohr magneton. The dependences $g_1(B_1)$ and $g_2(B_2)$ measured in the most important magnetic-field orientations ($\theta = 0°$ and $\theta = 90°$ with $\varphi = 0°,45°,90°$) are presented in Fig. 4. For a given magnetic-field orientation both values $g_1$ and $g_2$ turned out to be independent of the magnetic-field magnitude and thus to coincide with the values of $g_1^0$ and $g_2^0$ of the electron $g$ factors near the band minima corresponding to $X$ and $Y$ valleys. By changing angles $\theta$ and $\varphi$ we were able to measure $g_1^0(\theta,\varphi)$ and $g_2^0(\theta,\varphi)$. After denoting the principal axes of the $g$-factor tensor as $x,y,z$ one can easily derive the following formula that describes the angular dependences of the effective $g$ factor for a single valley:

$$(g^0)^2(\theta,\varphi) = \left[g_x^2 \cos^2\varphi + g_y^2 \sin^2\varphi\right] \sin^2\theta + g_z^2 \cos^2\theta, \quad (1)$$

where $g_x,g_y,g_z$ are the principal values of the $g$-factor tensor.

One of the principal axes of the $g$-factor tensors for both $X$ and $Y$ valleys coincides with the growth direction [001] for the symmetry reasons. It is convenient to denote this axis as $z$. According to Eq. (1), the principal value $g_z$ is measured directly in the case of $\theta = 0°$, and it equals $1.976 \pm 0.003$ for both valleys.

To identify the in-plane main axes of the $g$-factor tensor we plot two $g$-factor dependences $g(\theta = 90°,\varphi)$ on angle $\varphi$ in Fig. 5. Two branches $g_1^0(\varphi)$ and $g_2^0(\varphi)$ demonstrating twofold anisotropy are clearly resolved. These branches are shifted by the angle 90° one to another, and their extrema correspond to

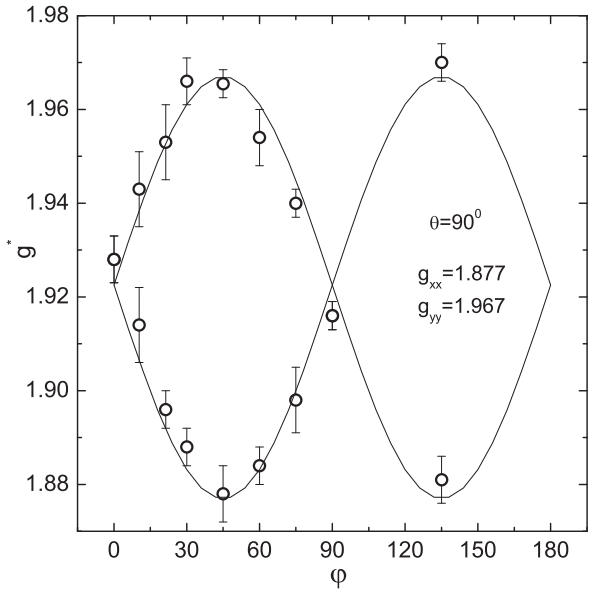


FIG. 5. The dependences of the effective $g$-factor $g^0$ and on $\varphi$ measured at the temperature of 1.5 K. Two values of $g^0$ at a single $\varphi$ correspond to two well-resolved ESR peaks. Angle $\theta$ was fixed at 90°. Solid lines represent fitting according to Eq. (1).

the values $\varphi = 45°, 135°$. Thus, the principal axes for both branches appear to be [100] and [010] as $\varphi$ is the angle between the in-plane magnetic field and the [110] direction. The result of fitting (solid line) the data in Fig. 5 according to Eq. (1) clearly justifies this assumption and enables us to measure the in-plane principal values $g_x = 1.877 \pm 0.005$ and $g_y = 1.967 \pm 0.005$ for a single valley. It is worth noting that we were unable to experimentally distinguish the $X$ and $Y$ valleys and thus it is impossible to determine which in-plane principal value of the $g$ factor corresponds to which in-plane crystallographic direction for a given single valley.

In conclusion, the electron spin resonance was studied in the asymmetrically doped to $n \sim 1.8 \times 10^{11}$ cm$^{-2}$ 16-nm AlAs quantum well grown in the [001] direction. We were able to detect the ESR even if the magnetic field was parallel to the 2DEG plane and thus to precisely investigate the in-plane anisotropy of the electron $g$ factor. If the magnetic field was perpendicular to the 2DEG plane or was aligned with the [110] or [1$\bar{1}$0] crystallographic axes only one ESR peak was found, whereas in all other cases two well-separated resonance peaks were observed. This fact clearly indicates that the in-plane $X$ and $Y$ valleys were occupied with electrons and each valley was characterized by the anisotropic $g$ factor with the [001], [010], and [001] principal axes. The principal $g$-factor values were extracted for each valley. Our data confirm also that the $Z$ valley is empty.

We gratefully acknowledge the financial support for the ESR measurements in AlAs from the Russian Science Foundation (Grant No. 14-12-00693) and cryogenic rotation stage development from the Russian Foundation for Basic Research.

[1] H. L. Stormer, Rev. Mod. Phys. **71**, 875 (1999).
[2] E. Wigner, Phys. Rev. **46**, 1002 (1934).
[3] E. C. Stoner, Rep. Prog. Phys. **11**, 43 (1947).
[4] M. Shayegan, E. P. De Poortere, O. Gunawan, Y. P. Shkolnikov, E. Tutuc, and K. Vakili, Phys. Status Solidi B **243**, 3629 (2006).
[5] E. P. De Poortere, Y. P. Shkolnikov, E. Tutuc, S. J. Papadakis, M. Shayegan, E. Palm, and T. Murphy, Appl. Phys. Lett. **80**, 1583 (2002)
[6] M. Schulte, J. G. S. Lok, G. Denninger, and W. Dietsche, Phys. Rev. Lett. **94**, 137601 (2005).
[7] K. Shen, M. Q. Weng, and M. W. Wu, J. Appl. Phys. **104**, 063719 (2008).
[8] S. Hallstein, M. Oestreich, W. W. Ruhle, and K. Kohler, *Proceedings of 12th International Conference High Magnetic Fields in the Physics of Semiconductors* (World Scientific, Singapore, 1996), p. 593.
[9] P. S. Eldridge, J. Hübner, S. Oertel, R. T. Harley, M. Henini, and M. Oestreich, Phys. Rev. B **83**, 041301(R) (2011).
[10] Yu. A. Nefyodov, A. V. Shchepetilnikov, I. V. Kukushkin, W. Dietsche, and S. Schmult, Phys. Rev. B **83**, 041307(R) (2011).
[11] Yu. A. Nefyodov, A. V. Shchepetilnikov, I. V. Kukushkin, W. Dietsche, and S. Schmult, Phys. Rev. B **84**, 233302 (2011).
[12] V. K. Kalevich and V. L. Korenev, Pis'ma Zh. Eksp. Teor. Fiz. **57**, 557 (1993) [JETP Lett. **57**, 571 (1993)].
[13] Zh. A. Devizorova and V. A. Volkov, Pis'ma Zh. Eksp. Teor. Fiz. **98**, 110 (2013) [JETP Lett. **98**, 101 (2013)].
[14] Zh. A. Devizorova, A. V. Shchepetilnikov, Yu A. Nefyodov, V. A. Volkov, and I. V. Kukushkin, Pis'ma Zh. Eksp. Teor. Fiz. **100**, 111 (2014) [JETP Lett. **100**, 102 (2014)].
[15] D. Stein, K. V. Klitzing, and G. Weimann, Phys. Rev. Lett. **51**, 130 (1983).
[16] C. Kallin and B. I. Halperin, Phys. Rev. B **30**, 5655 (1984)
[17] A. Berg, M. Dobers, P. R. Gerhardts, and K. von Klitzing, Phys. Rev. Lett. **64**, 2563 (1990).
[18] E. Abrahams, Physica E **3**, 69 (1998).